POAC'13
Espoo, Finland

Proceedings of the 22nd International Conference on
Port and Ocean Engineering under Arctic Conditions
June 9-13, 2013
Espoo, Finland

RUBBLE ICE TRANSPORT ON ARCTIC OFFSHORE STRUCTURES (RITAS), PART II: 2D SCALE-MODEL STUDY OF THE LEVEL ICE ACTION

Nicolas Serré [1], Wenjun Lu [2], Knut Høyland [2], Basile Bonnemaire [1], Juliane Borge [1], Karl-Ulrich Evers [3]

[1] Multiconsult, Tromsø, NORWAY

[2] Sustainable Arctic Marine and Coastal Technology (SAMCoT), Centre for Research-based Innovation (CRI), Norwegian University of Science and Technology, Trondheim, NORWAY

[3] HSVA, Hamburg, GERMANY

ABSTRACT

A model scale experiment on the interaction between level ice and an arctic offshore structure with a downward bending hull was conducted in April 2012 in the large ice tank of HSVA. The experiments investigate the different mechanical processes contributing to the ice action. The present paper is completed by a companion paper "*Rubble Ice Transport on Arctic Offshore Structures (RITAS), part I: Model scale investigation of level ice action mechanisms*". Detailed investigations on special aspects of the level ice action mechanisms are presented in "*Rubble Ice Transport on Arctic Offshore Structures (RITAS), part III: Analysis of scale model rubble ice stability*" and "*Rubble Ice Transport on Arctic Offshore Structures (RITAS), part IV Tactile sensor measurement of the level ice load on inclined plate*".

The structure, a so called buoyancy box, is inclined at the waterline and promotes a downward bending failure of the level ice. Two-dimensionality is introduced by limiting the panel width to 1 meter with two transparent Lexan plates allowing monitoring of the ice breaking and accumulation process. Several parameters are varied: ice thickness, ice density, ice velocity. A tactile sensor is installed on the ice breaking area of the structure to monitor the local waterline ice loads. During each interaction tests, the volume and buoyancy of the rubble accumulated on the structure are measured for derivation of the rubble porosity. The waterline ice load is oscillating. The experimental results show that the magnitude of the load peaks increases. The rubble is subjected to a rotating motion and to a series of collapse events. Increased buoyancy forces reduce the rubble porosity.

INTRODUCTION

The level ice action on offshore structures can generally be reduced by designing the structure geometry such that a bending failure of the level ice is promoted. The breaking of ice on large structure produces subsurface rubble ice accumulating under the incoming level ice and travelling along the structure's hull. The effect from the rubble transport on the waterline ice load on a flat downward sloping hull has been studied in Serré et al. (2013) as well as the influence from ice density, thickness, velocity and incidence. It was observed that the rubble accumulation influences the waterline ice load until a certain limit, above which additional rubble does not anymore increase the waterline ice load. On the contrary, ISO 19906 (2010) suggests that the ice breaking load (related to the waterline ice load) can be discomposed in 5 components, and 3 of them are dependent on the amount of subsurface rubble, i.e. their magnitude increases as long as the amount of subsurface rubble increases. These 3 components are H_P, the load required to push the ice sheet through the ice rubble, H_R, the load to push the ice blocks down the slope through the ice rubble, and H_L, the load required to press down the ice rubble beneath the advancing ice sheet prior to breaking it (Croasdale, 1980; Croasdale et al., 1994). The two other components of the ice breaking action are H_B, the ice breaking load, and H_T, the load to turn the ice block at the bottom of the slope. The contradiction between the experimental results and the conceptual model shows that the ice action mechanisms are not yet entirely understood and thus may, at times, lead to an inaccurate modelling of the ice action.

The experiment described in the present paper was designed in order to investigate the mechanical processes contributing to the level ice action on a wide downward sloping structure. The 3D case was studied in RITAS part I (Serré et al., 2013). In the present article, the ice breaking and accumulation pattern is studied in 2D such that it is possible to observe the ice motion within a cross-section of the subsurface rubble, and verify how it compares to the ISO description. A similar 2D test investigating the broken ice load on an inclined plate is reported in Timco (1991) with monitoring of the underwater ice motion and ice load distribution vertically along the plate. Load from level ice breaking on an upward inclined structure was later investigated in a 2D setting by Paavilainen et al. (2011; 2013). The current work focuses on level ice interaction with downward sloping structure and investigates the physical properties of the rubble ice, the rubble motion and the load distribution in the waterline region. The buoyancy box is further used for determination of the mechanical properties (Kulyakhtin et al., 2013) of the subsurface rubble. The physical properties comprise the buoyancy and porosity, while the mechanical properties here refer to ice rubble Mohr-Coulomb parameters.

The present paper (RITAS part II) describes the experimental set up, the ice breaking process, the rubble motion into the box and the porosity computations. Part III (Kulyakhtin et al., 2013) derives the rubble mechanical properties from stability tests. Part IV (Lu et al., 2013) is a description of tactile sensors measurements of the waterline ice load onto the inclined part of the buoyancy box.

EXPERIMENTAL SET UP

Procedure

The buoyancy box interacts with 5 level ice sheets. The back of the box is inclined at the waterline and the ice breaking load on the inclined plate is measured with a tactile sensor. The accumulation of subsurface rubble into the box is monitored with underwater video-cameras during the entire interaction. The buoyancy of the accumulated rubble is measured at the end of the interaction by measuring the weight of the submerged box filled with rubble and computing the difference with the weight of the submerged empty box. The weight of the box submerged in the water is measured with a load cell fixed to a crane hook.

Buoyancy box

A buoyancy box is built according to the design given in Figure 1. The back of the box is made of the same material as the structures tested in Serré et al. (2013) and the sides are made of Lexan plates. The back wall comprises an inclined portion at the waterline, a vertical portion and an ice spoiler (similar geometry as the structures). The box is mounted on a support frame which is fixed to the service carriage (Figure 2 a).

The ice crushing on the box's frame is prevented by the installation of "ice knives", i.e. sharp steel edges cutting through the ice. The distance between the knives is 940 mm.

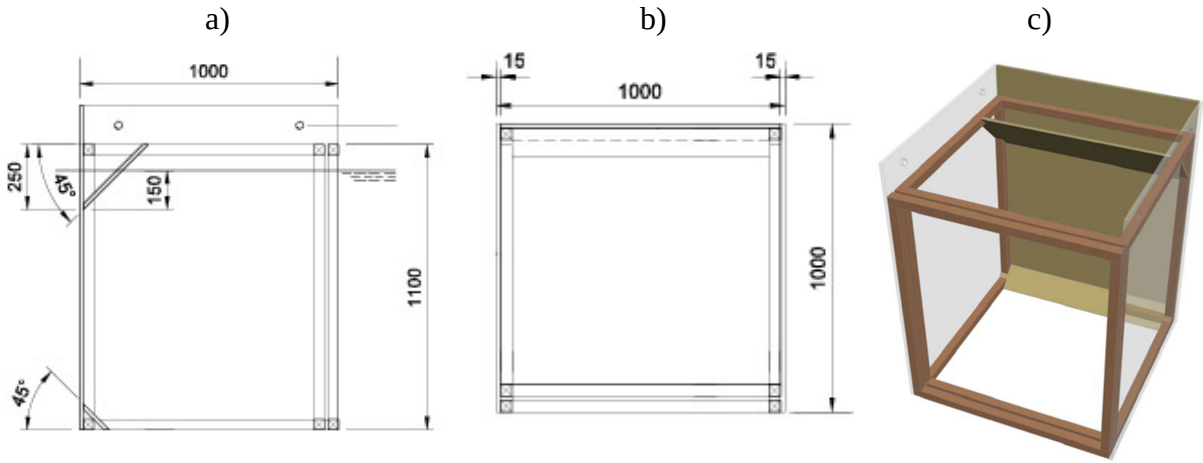

Figure 1 Technical drawing of the buoyancy box, in a) from side, in b) from above, in c) 3D drawing.

Load measurement

The inclined plate at the waterline is covered with a tactile sensor and a protection film for measurement of local ice loads. The position of the tactile sensor on the inclined plate is given in Figure 2 b). The weight of the box is measured by lifting the box with the ice basin roof crane. A load cell is mounted on the crane hook.

a) b)

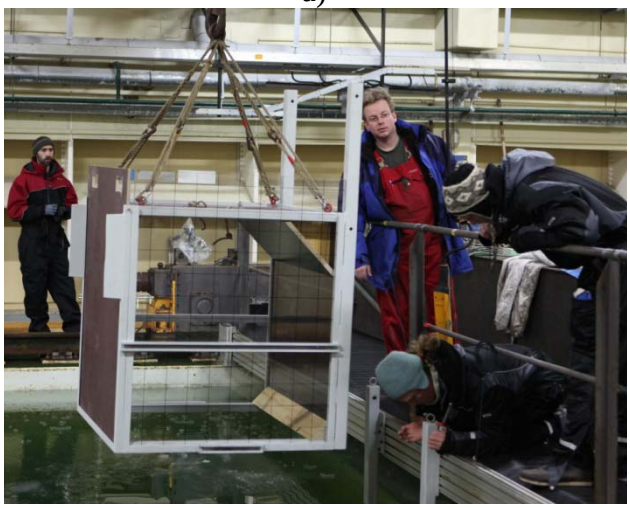

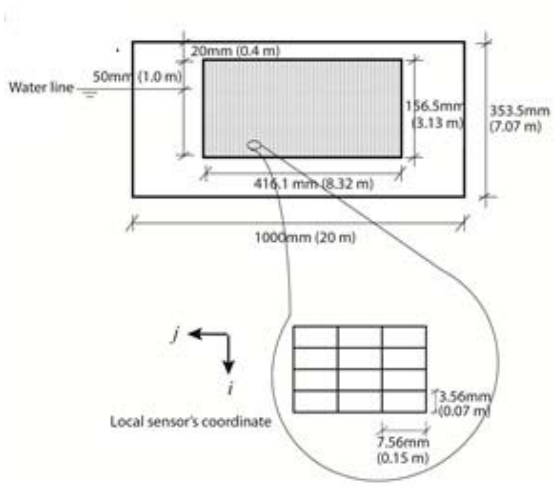

Figure 2 In a) buoyancy box being attached to the service carriage, front door and roof are removed during the interaction test. In b) tactile sensor position on the inclined plate (Lu et al., 2013).

Ice characteristics

For each test series, the buoyancy box interacted with model level ice. The ice characteristics are measured according to the methods described in Schwarz et al. (1981) and Evers and Jochman (1993). The ice characteristics are given in Table 1.

Table 1. Ice properties for the different ice sheets

Parameter	**Unit**	**Test 1000**	**Test 2000 (High velocity)**	**Test 3000 (Low density)**	**Test 4000 (High thickness and E module)**	**Test 5000**
Ice thickness	cm	4.3	4.3	4.7	6.1	4.1
Flexural strength	kPa	53	58.2	54.6	45.7	47.1
Elastic modulus	MPa	61	53	88	103	31
Ice-wood friction				0.018		
Ice-tactile sensor friction				0.027		
Ice density	kg/m^3	906	902	806	928	894
Ice salinity	‰	Approximately 3.5				
Water density	kg/m^3	1006				
Water salinity	‰	6.9				

Test matrix

The buoyancy box tests included several steps: interaction with level ice and ice load measurements, measure weight of box filled with rubble ice from the interaction, and stability tests. All test numbers are listed in Table 2.

Table 2. Level ice buoyancy box tests

Test #	Action	Description	Ice drift length [m]	Velocity [m/s]
Ice sheet 1 and 2 (x = 1,2)				
X210	Buoyancy box filling	Pushing buoyancy box until filled with ice, tactile sensor measurement of ice load (in test 2210).	10 (20 in 2210)	0.045 (0.2 in 2210)
X220	Measurements	Sinking buoyancy box		
X230	Rubble stability	Tilting buoyancy box		
Ice sheet 3 and 4 (x = 3,4)				
X210	Buoyancy box filling	Pushing buoyancy box 10 m into the ice	10	0.045 (0.02 in 4210)
X211	Buoyancy box filling	Pushing buoyancy box 10 m into the ice	10	0.2
X212	Buoyancy box filling	Pushing buoyancy box 10 m into the ice	10	0.045
X220	Measurements	Sinking buoyancy box		
X230	Rubble stability	Tilting buoyancy box		
Ice sheet 5				
5210	Buoyancy box filling	Pushing buoyancy box 9 m into the ice	9	0.045
5220	Measurements	Sinking buoyancy box		
5230	Rubble stability	Tilting buoyancy box		
5240	Buoyancy box filling	Pushing buoyancy box 3 m into the ice, with roof, no tactile sensor	3	0.045
5241	Measurements	Sinking buoyancy box		
5250	Buoyancy box filling	Pushing buoyancy box 3 m into the ice, with roof, no tactile sensor, box full at start	3	0.045
5251	Measurements	Sinking buoyancy box		
5260	Buoyancy box filling	Pushing buoyancy box 3 m into the ice, with roof, no tactile sensor, box full at start	3	0.045
5261	Measurements	Sinking buoyancy box		

Video monitoring

A grid is painted on the Lexan plates. The grid squares are 10 x 10 cm. The rubble accumulation into the box is recorded by two video cameras placed underwater on each side of the box.

RESULTS

Ice interaction process

During motion of the buoyancy box into the level ice, the ice penetrates into the buoyancy box and is subjected to the following process:

- Bending failure of level ice on the inclined plate
  - The size of the broken blocks tends to decrease during the interaction (Figure 3)
  - After enough rubble has accumulated, a further breaking occurs at the vertical wall (Figure 4)
- Downward sliding of broken ice blocks along the back side of the box
- Uplifting of the blocks and accumulation under the incoming level ice
- The rubble accumulation rotates due to the level ice motion.
- The rubble accumulation increases in size and collapses regularly (Figure 5)

a) b)

Figure 3. Decreasing block size during the interactions, here test run 5210, in a) a large beginning of interaction level ice block is highlighted; in b) a large end of interaction ice block is highlighted.

a) b)

Figure 4. Further breaking on the vertical wall during test run 5210, in a) one ice block spans from the inclined wall to the vertical wall; in b) the block has broken (fracture in red circle).

a) b)

Figure 5. Collapse event during test run 5210, 120 s; in a) the rubble reaches a maximum depth; in b) the rubble has just collapsed and extends further away from the inclined panel.

During the test series 4000, cracks in the level ice initiated from the ice knives. A large proportion of the level ice interacting with the inclined planed was already broken.

Rubble volume

The volume of ice accumulated in the buoyancy box is measured from the underwater videos (Figure 6) and is composed of:

- Level ice, being the ice layer floating at the waterline and the ice layer resting against the back wall of the box,
- Ice rubble, accumulated under the level ice. It is composed of water and ice.

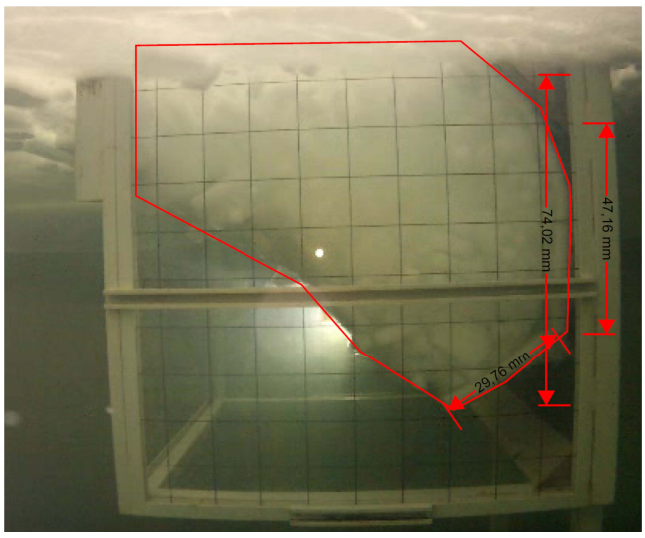

Figure 6. Measurement of volume of accumulated rubble, test run 5210 (end).

The evolution of the ice rubble together with the level ice volume in function of the penetration distance of the buoyancy box into the level ice is given in Figure 7. The volume of ice into the box at the end of the interaction is given in Table 3. A small quantity of ice escaped from the box during the interaction. The oscillations of the measured volume of rubble are caused by uncertainty of the measurement method which is estimated to 0.03 m^3.

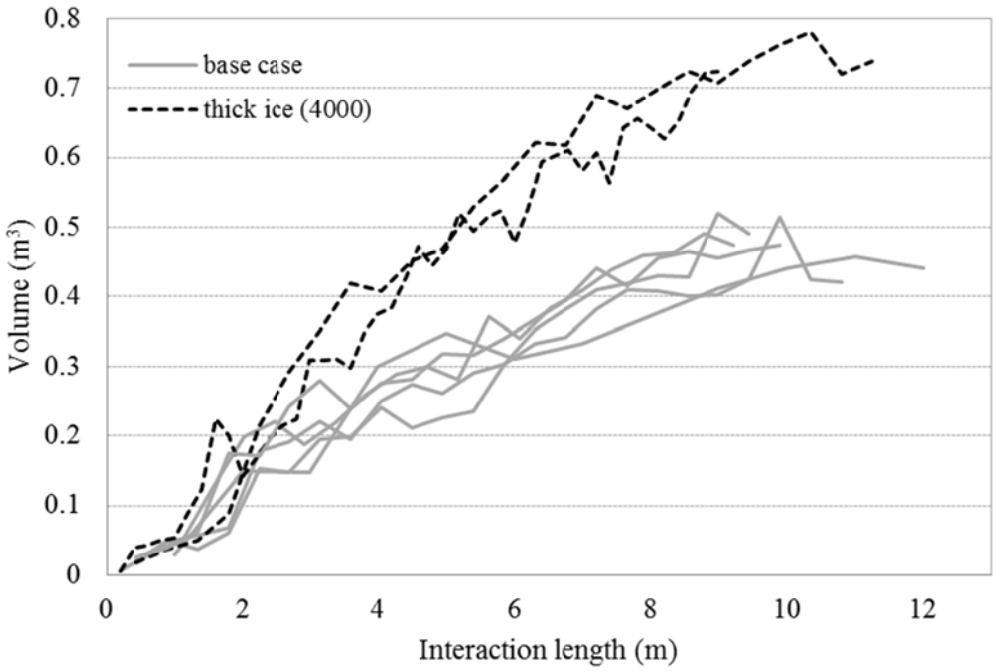

Figure 7. Volume of ice rubble + level ice into the box, as a function of the penetration of the buoyancy box into the level ice. Black dashed lines are high thickness and E module tests (4210, 4212) and grey lines are tests with base case thickness (4.3 – 4.7 cm) and velocity (0.045 m/s).

Buoyancy and porosity

The results from the buoyancy measurements are presented in Table 3 together with the computed porosities. The macro-porosity of the sub-surface rubble accumulated under the level ice is computed with Eq.(1),

$$\eta = \frac{B / g - (\rho_w - \rho_i)(V_r + V_{LI})}{V_r (\rho_i - \rho_w)} \quad (1)$$

where η is the rubble porosity, V_r is the volume of ice rubble (ice + water), V_{LI} is the volume of level ice inside the box (at waterline + along the back panels), B is the box buoyancy, g is the gravity coefficient.

Table 3. Results from buoyancy measurements of the buoyancy box

Test #	Submerged box weight (N)	Buoyancy (N)	Ice rubble volume (m^3)	Porosity
Submerged box in open water	-600	-	-	-
Submerged box in open water with 40 kg weights	-940.9		-	-
1220	-277.2	323	0.35	0.26
2220	-187.6	412	0.46	0.27
3220 (added 40 kg)	-173.1	768	0.40	0.21
4220 (added 40 kg)	-560.8	380	0.62	0.39
5220	-210.4	390	0.41	0.25
5241	-469.3	131	0.13	0.38
5251	-345.5	255	0.25	0.26
5261	-265.2	335	0.37	0.32

Ice load

A typical example of the total ice load on the tactile sensor is given in Figure 8 (test run 5210). The time series is composed of peaks and the load can return to 0 between the peaks. The period with no load is referred as “no-load event”. In all tests except test run 2210 (high velocity and 20 m travel distance) the magnitude of the peaks increased during the interaction. There were no events with zero load during the high velocity tests (continuous ice contact on the tactile sensor), except during the large ice thickness tests (series 4000). In series 4000, both the larger ice thickness and the observed breakage of the level ice at the entrance of the box could explain the continuous presence of no-load events.

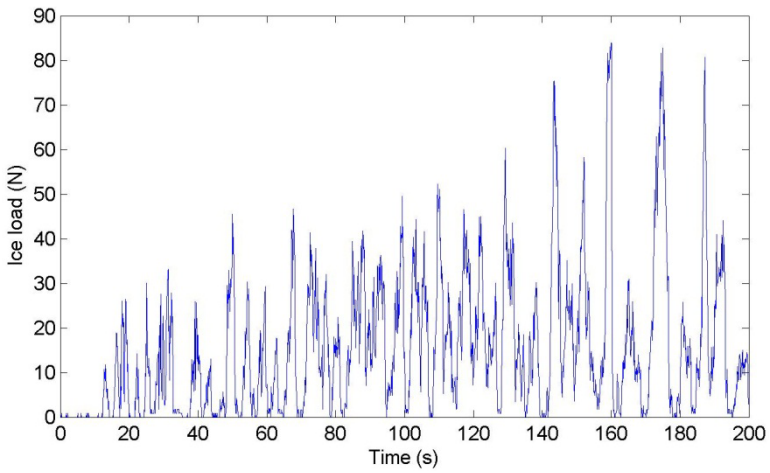

Figure 8. Total ice load on tactile sensor, test run 5210.

The maximum load registered by the tactile sensor is given in Table 4.

Table 4. Maximum total load on tactile sensor.

Test run	**2210**	**3210**	**3211**	**3212**	**4210**	**4211**	**4212**	**5210**
Peak load (N)	225	160	225	200	105	300	190	85

DISCUSSION

Rubble porosity

The evolution of the porosity with the volume of accumulated rubble can be determined in test series 5000 where the buoyancy of accumulated rubble was measured each 3 meters of a 9 meters level ice interaction with the buoyancy box (test run 5240, 5250, and 5260). The measurements show that the porosity was highest at the beginning of the interaction, when 3 meters of level ice have penetrated into the box (porosity 0.38, run 5241). By increasing the volume of rubble ice with 3 m of level ice, the porosity decreases to 0.26 (run 5251). The porosity increases to 0.32 with 3 additional meters of level ice into the box is not explained. This result is however lower than the porosity in test 5241. Considering the measurement uncertainties it does not contradict with the hypothesis of a decreasing porosity for an increase in rubble volume.

The effect of the rubble amount on the porosity can be explained by a larger amount of rubble causing higher buoyancy forces and thus compaction in the rubble, which leads to reduction of the porosity. This hypothesis corresponds to the results in Figure 9, where the porosity decreases in the buoyancy tests showing higher buoyancy. The test with the lowest porosity is the test with the lowest ice density (run 3212). The highest porosity is measured in the test run 4212 (large ice thickness).

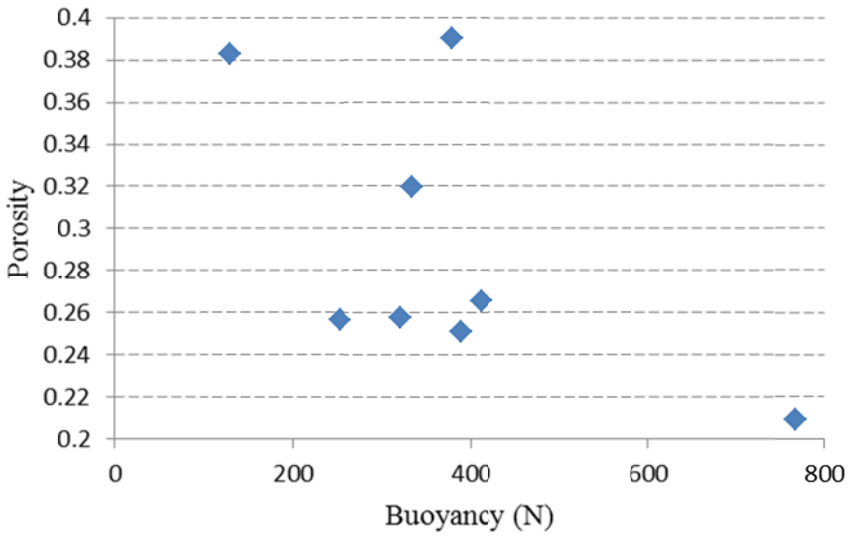

Figure 9. Porosity in function of rubble buoyancy, from results in Table 3.

Influence of rubble amount on waterline ice load

The increasing magnitude of the waterline ice load peaks show that the waterline ice load is influenced by the amount of accumulated rubble. The largest load peaks are never located in

the beginning of the experiments, and the largest peak loads at the end of the experiment are more than twice larger than the largest peaks from the interaction start.

The load curves recorded by the tactile sensor also show that the time interval between the no-load events increases during the interaction time, and thus with increasing volume of accumulated rubble. The underwater videos show that no-load events can occur when the tactile sensor loses contact with the ice: due to the tilting motion of the broken ice blocks, the lower edge of a broken block can be below the tactile sensor before the upper edge has reached the sensor at the waterline. The distance between the two edges of one block is related to the breaking length. No-load events can occur when the breaking length is larger than the length of the tactile sensor under the waterline (106 mm, Figure 2 b).

The rubble accumulation also causes resistance to the broken ice blocks rotation at the transition point between the inclined and the vertical portion of the hull, adding a resistance component to the ice turning process described by H_T in Croasdale et al. (1994). The present experiment shows that above a certain amount of accumulated rubble, the ice blocks further break at this transition point.

A third contribution from the rubble to the waterline ice load is the increased buoyancy force on the downward bending and downward sliding ice sheet, respectively H_L and H_R in ISO 19906 (2010). H_L also includes the load necessary to fracture the rubble accumulation along a vertical failure plane under the ice edge. This failure mode was not observed during the experiments, where the rubble was continuously rotating. Similar observation has also been made by Timco (1991).

CONCLUSION

A 2-dimensional experiment on the downward breaking of a level ice sheet on a structure was performed in the HSVA model ice basin. The ice thickness, density and velocity were varied between the ice sheets. The broken level ice slided downward along the structure and formed an accumulation of subsurface rubble. The waterline ice load, rubble volume, buoyancy and porosity were measured. The breaking process was compared to the ISO 19906 formulation.

The following mechanisms were observed accordingly to the ISO 19906 formulation:

- The waterline ice load increases when the size of the rubble accumulation increases.
- A lower ice density and a larger ice thickness caused higher waterline ice loads.

The following mechanisms were observed and are not considered in the ISO 19906 formulation:

- Further ice breaking is observed during the ice turning phase on the vertical wall.
- The rubble rotates continuously and the accumulation presents regular cycles of growth and collapse.

The porosity results are affected by measurement uncertainty but tend to show that:

- A higher buoyancy force reduces the porosity.
- Accordingly, the porosity tends to decreases when the size of the accumulation increases.

ACKNOWLEDGMENT

This project required the help of many participants who deserve the deepest acknowledgments: NTNU participants Hening Helgøy, Sergey Kulyakhtin and colleagues at Multiconsult Oda Skog Astrup, Trine Lundamo, Hege Nilsen, and Arnor Jensen. This experiment could be realised thanks to Arne Gürtner (Statoil) who financed the experimental set-up. The authors would also like to acknowledge the Norwegian Research Council through the project 200618/S60-PetroRisk and the SAMCoT CRI for financial support and all the SAMCoT partners.

The work described in this publication was supported by the European Community's 7th Framework Programme through the grant to the budget of the Integrated Infrastructure Initiative HYDRALAB-IV, Contract no. 261520. The authors would like to thank the Hamburg Ship Model Basin (HSVA), especially the ice tank crew, for the hospitality, technical and scientific support and the professional execution of the test programme in the Research Infrastructure ARCTECLAB.

REFERENCES

Croasdale, K.R., 1980. Ice forces on fixed, rigid structures. In: CRREL Special Report 80-26, Working Group on ice forces on structures. A State-of-the-Art Report. Int. Association for Hydraulic Research, Section on ice problems. U.S. Army CRREL, Hanover, NH, USA, pp. 34-103.

Croasdale, K.R., Cammaert, A.B. and Metge, M., 1994. A Method for the Calculation of Sheet Ice Loads on Sloping Structures. Proc. 12th Int. Symposium on Ice, The Norwegian Institute of Technology, Trondheim, Norway, August 23-26, Vol. 2, pp. 874–875.

Evers, K-U and Jochman, P., 1993. An advanced technique to improve the mechanical properties of model ice developed at the HSVA ice tank. Proceedings of the 12nd International Conference on Port and Ocean Engineering under Arctic Conditions, Hamburg, Germany, pp. 877-888.

ISO/FDIS 19906, 2010. Petroleum and natural gas industries – Arctic offshore structures, ISO TC 67/SC 7. Final Draft International Standard, International Standardization organization, Geneva, Switzerland, 434p.

Kulyakhtin, S., Høyland, K., Astrup, O., Evers, K-U., 2013 Rubble ice transport on arctic offshore structures (RITAS), part III: analysis of model scale rubble ice stability. Proceedings of the 22nd International Conference on Port and Ocean Engineering under Arctic Conditions, Espoo, Finland.

Lu, W., Serré, N., Evers, K-U., 2013. Rubble Ice transport on Arctic Offshore Structures (RITAS), part IV Tactile sensor measurement of the level ice load on inclined plate. Proceedings of the 22nd International Conference on Port and Ocean Engineering under Arctic Conditions, Espoo, Finland.

Paavilainen, J., Tuhkuri, J. and Polojärvi, A., 2011. 2D numerical simulations of ice rubble formation process against an inclined structure. Cold Regions Science and Technology, 68(1–2): 20-34.

Paavilainen, J. and Tuhkuri, J., 2013. Pressure distributions and force chains during simulated ice rubbling against sloped structures. Cold Regions Science and Technology, 85(0): 157-174.

Schwarz, J., Frederking, R., Gavrillo, V., Petrov, I.G., Hirayama, K., Mellor, M., Tryde, P. and Vaudrey, K.D., 1981. Standardized Testing Methods for Measuring Mechanical Properties of Ice; Cold Regions Science and Technology, Vol. 4, pp. 245-253.

Serré, N., Høyland, K., Lundamo, T., Bonnemaire, B., Evers, K-U. and Gürtner, A., 2013. Rubble Ice transport on Arctic Offshore Structures (RITAS), part I: Scale-model investigations of level ice action mechanisms. Proceedings of the 22nd International Conference on Port and Ocean Engineering under Arctic Conditions, Espoo, Finland.

Timco, G., 1991. The vertical pressure distribution on structures subjected to rubble forming ice, 11th International Conference on Port and Ocean Engineering under Arctic Conditions, St.John's, Canada, pp. 185-197.